Numerical Simulation of ECR Plasma in Air Breathing Ion engine (ABIE): Neutral Gas Density Distribution and ECR Plasma Formation

IEPC-2015-454p／ISTS-2015-b-454p

Presented at Joint Conference of 30th International Symposium on Space Technology and Science
34th International Electric Propulsion Conference and 6th Nano-satellite Symposium,
Hyogo-Kobe, Japan
July 4 – 10, 2015

Tsubasa Yasukochi[1]
Graduate School of Engineering, Kobe University, Kobe, 657-8501, Japan

Hideyuki Usui*[2], Yohei Miyake*[3]
Graduate School of System Informatics, Kobe University, Kobe, 657-8501, Japan

Shinichiro Kawaguchi[4]
Graduate School of Engineering, Kobe University, Kobe, 657-8501, Japan

Masato Fukuda[5]
Graduate School of System Informatics, Kobe University, Kobe, 657-8501, Japan

and

Kumiko Yokota[6], Masahito Tagawa*[7]
Graduate School of Engineering, Kobe University, Kobe, 657-8501, Japan

**Corresponding authors*

Abstract: Formation of the electron cyclotron resonance (ECR) plasma in air breathing ion engine (ABIE) was numerically simulated using computational code called electromagnetic spacecraft environment simulator (EMSES) in order to optimize the design of ABIE. Electron and ion density distributions in the plasma chamber were calculated with three different configurations of antenna, magnets and metal boundaries. It was suggested for efficient ion generation that the configuration in which antenna and magnet are located perpendicular to each other increases the ion generation. The effect of metal boundaries is observed by forming the ECR plasma. Separate simulations focusing on the dynamics of neutral particles were also performed by taking into account their scattering at the reflector surface of ABIE. It was analyzed that the use of trapping desorption process which is one of the scattering process is advantageous for ABIE.

[1] Graduate student, Department of Engineering, 150t376t@ stu.kobe-u.ac.jp
[2] Professor, Department of System Informatics, h-usui@port.kobe-u.ac.jp
[3] Research associate, Department of System Informatics, y-miyake@eagle.kobe-u.ac.jp
[4] Graduate student, Department of Engineering, 147t330t@stu.kobe-u.ac.jp
[5] Graduate student, Department of System Informatics, 159x224x@stu.kobe-u.ac.jp
[6] Research associate, Department of Engineering, yokota@mech.kobe-u.ac.jp
[7] Associate professor, Department of Engineering, tagawa@mech.kobe-u.ac.jp

Nomenclature

B	=	dipole magnetic field strength
E	=	electric field strength
f	=	power frequency
I_l	=	electron density (or intensity)
L	=	grid spacing
m	=	mass of the electron
m_d	=	magnetic field
n_s	=	initial electron density
n_t	=	neutral particle density
P_i	=	collision probability of electrons per unit time Δt
q	=	mass of the electric charge
r	=	position vector from the center of magnetic field
v	=	velocity of the electron
v'	=	collision frequency
v_s	=	initial electron velocity
v_i	=	velocity of the incident electron
x_i	=	beam direction
σ	=	cross-section of election/neutral collision

I. Introduction

THE air breathing ion engine (ABIE) is a new concept for an ion engine, which uses neutral gases in the upper atmosphere as a propellant instead of conventional xenon. The ABIE concept was proposed by Nishiyama in 2003[1], and the system study was updated in 2004[2]. Because the thrust of an ABIE increases with increasing density of the incoming gas, the ABIE is suitable for compensating drag for low altitude satellites. In conjunction with the recent trend to develop a super-low altitude satellite, which is orbiting at the altitude of 150–200 km, the ABIE is considered to be an ideal thruster to compensate the atmospheric drag and it is considered as a key technology for developing close but new frontier in space. Although most of prior works on ABIE have been conducted in a theoretical manner, some numerical studies using Monte Carlo simulations focused on the air intake of ABIE, as reported by Fujita[3,4]. He concluded that ABIE is feasible in the altitude range 140–200 km. There also be some other conceptual works for ABIE[5-7]. However detailed studies focusing on a specific design have not been reported. On the other hand, experimental study faced technological difficulties for simulating the neutral gas environment at super-low altitude orbits with ground-based facilities. The main issue is on the difficulty in the formation of the 8 km/s "continuous" flow of atomic oxygen or nitrogen molecule. Tagawa et al. applied a "pulsed" hyperthermal 8 km/s N^2 flow to the ABIE study[8]. They demonstrated the ECR plasma formation with 8 km/s N^2 pulse formed by a laser detonation hyperthermal beam source, which has been used for atomic oxygen-induced material degradation studies in space. In contrast, Hisamoto et al. reported a "continuous" beam using ECR microwave ion engine technique. However, the translational energy of atomic oxygen beam, which is electrostatically accelerated before neutralization, is too high for simulating 8 km/s[9]. Due to the difficulty of the experimental approach to ABIE, combined use of theoretical and experimental approaches is indispensable.

In this study, two types of simulations were performed. One is an ECR plasma simulation inside the discharge chamber of μ6 ion engine, which was used for the experimental study of ABIE. The other is a simulation of atom/molecule trajectories reflected at the reflector surfaces. The latter simulation was performed for concentrating the neutral atoms at the ion generation area in the discharge chamber. The purpose of this simulation is to study the design guideline of ABIE to achieve a low-pressure operation capability, which enables to extend the operational altitude range.

II. Numerical ECR simulation method

A) Simulation method

The simulation code used in this simulation is electromagnetic spacecraft environment simulator (EMSES) which is based on the Maxwell's equations for electromagnetic fields reaction and the equation of motion for a large number of macro-particle with the FDTD scheme and the Newton's law for thermions of plasma particles. This simulation code has been developed for the self-consistent analysis of the spacecraft-plasma interactions[10].

Characteristic feature of EMSES is the time-dependent electromagnetic field update based on the kinetic plasma motions in the simulation space[11].

B) The ion generation model and the dipole moment model

Previous study developed the ion generation algorism in the EMSES based on the MCC model. The electron density in the plasma is gradually decreased by electron-atom collisions. Change in the electron density through electron-atom collision is given by the equation (1);

$$dI_1 = -\sigma I_1 n_t dx \tag{1}$$

σ is the cross-section of the electron-atom collisional reactions which depends on the collision energy. The cross-section is expressed as the function of the sum of the kinetic energy of the intake particle. The amount of the cross-section between the intake particle and the neutral particle is expressed by the sum of the cross-section for each kind of the collisions between them.

The collisional processes between electron and atoms such as ionization or scattering were categorized by the value of P_i is expressed by (2), v_1 is velocity of the incident electron, n_t is neutral particle density, x_i is the beam direction.

$$P_i = 1 - \exp(-\Delta t v_i \sigma n_t(x_i)) \tag{2}$$

In the EMSES, we defined dipole magnetic field given by Equation (3).

$$B_{dipole} = (3 \times \frac{md \cdot r}{r^5} \cdot r - \frac{md}{r^3}) \tag{3}$$

r is a position vector from the center of magnetic field, and md is dipole moment vector. In order to reflect magnetic field to plasma dynamics, the magnetic field distribution over the computational area was calculated. All plasma particles in the simulation space follow the magnetic field distribution in the equations of motion shown in Equation (4)[7].

$$\frac{dv}{dt} = \frac{q}{m}(E + v \times (B + B_{dipole})) \tag{4}$$

C) Simulation model

The ABIE simulation was carried out in the simulation space in 108 × 108 × 108 grids. The simulation model of ABIE used in this study was based on the design of experimental model used in our previous study[8]. Figure 1 (a) shows the discharge chamber of the ABIE simulated in the model, which includes a rod antenna and magnets. Figures 1 (b) - (d) show the three configurations of the antenna, magnets and metal boundary calculated in this study. The dipole antenna located at the center of discharge chamber was consisted in two 5-grid-long electrically conducting rods with a 2-grids spacing. Two magnets are located 20 grids from center position. The cylindrical metal boundaries (reflectors) with 40 grids in diameter are placed on the xy planes at z=0 and 108. Table 1 lists the simulation parameter used in this simulation. All calculations in this study were carried out by the supercomputer at the Institute for Information Management and Communication, Kyoto University.

Table 1 Simulation parameters used in this study.

Parameter	Value
Time step (Δt)	1.7E-12 (s)
Grid spacing (L)	5E-3 (cm)
Initial electron density (n_s)	1.7E6 (1/m³)
Initial electron velocity (v_s)	0 (eV)
Collision frequency (v')	0 (1/s)
Power frequency (f)	3 (GHz)
Power (P)	35 (w)
Magnetic field (m_d)	3400 (T)

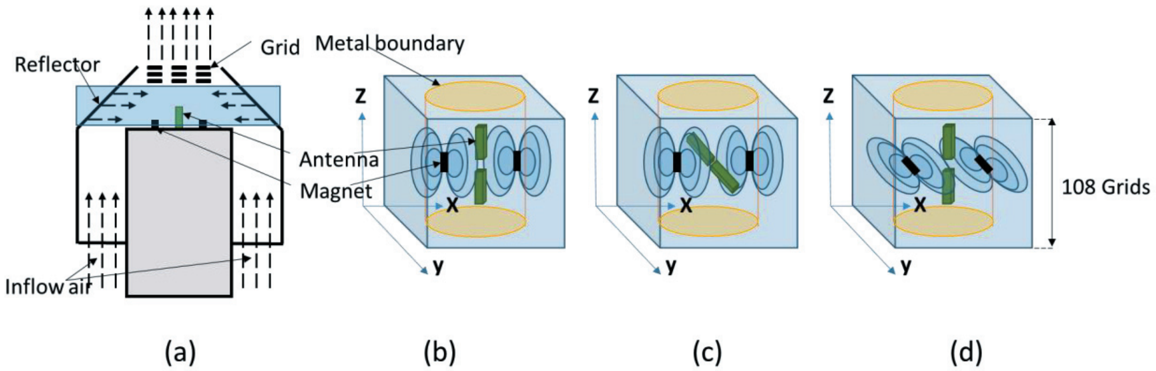

Figure 1. Configuration of ABIE simulated in the model (a) and antenna and magnet configurations in the discharge chamber calculated in this study (b)-(d). (b): y-direction antenna and y-direction magnet, (c): z-direction antenna and y-direction magnet, and (d): y-direction antenna and z-direction magnet. Metal boundaries are located in xy-plane.

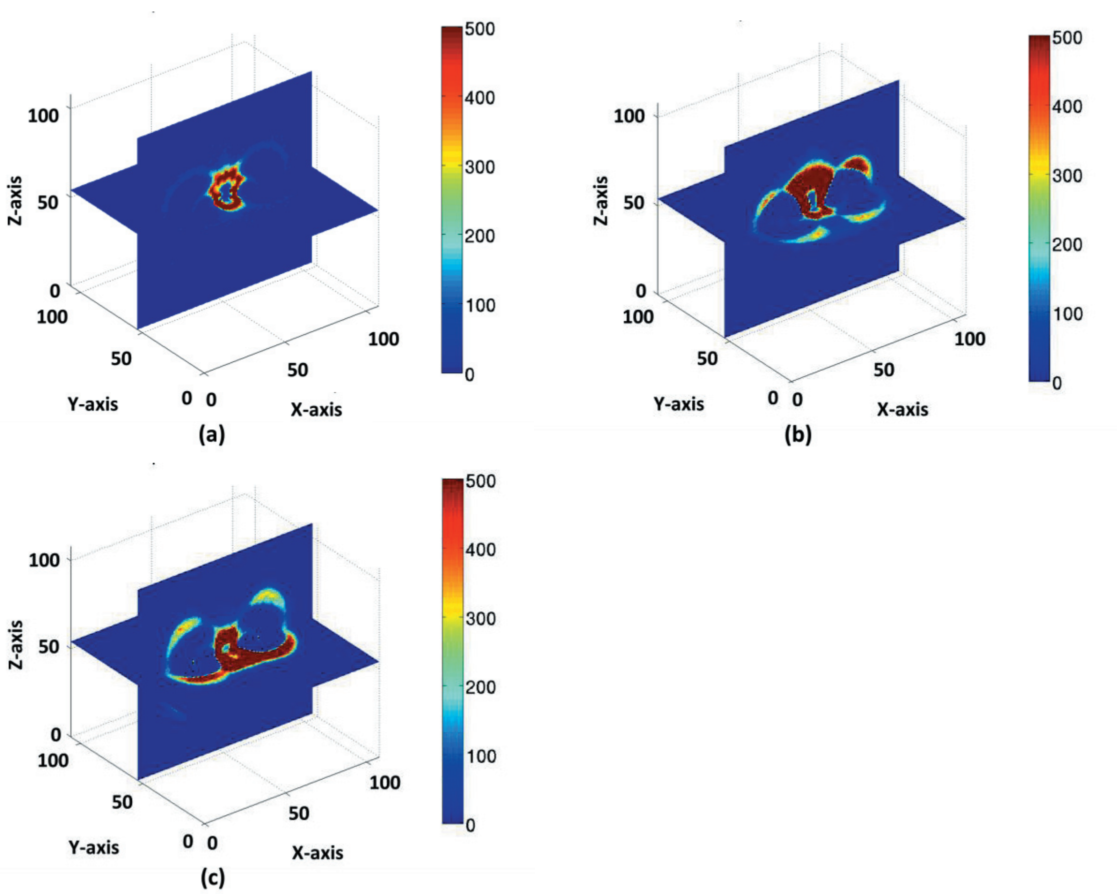

Figure 2. Ion density distributions. (a): y-direction antenna and y-direction magnet, (b): z-direction antenna and y-direction magnet, and (c): y-direction antenna and z-direction magnet. Metal boundaries are located in xy-plane.

III. Results and Discussion

A. ECR plasma simulation

Figures 2(a) - 2(c) show the ion density distributions in the configurations shown in Figures 1(b) to 2(d), respectively. The spatial distributions of ion shown in Figure 2 are the snapshot taken at t=13 μs. The figure displays the ion density at the cross-sections on the planes at y=54 and z=54. It is obvious that ions are generated only at the vicinity of the antenna in the case of the configuration shown in Figure 2(a). In contrast, ions are generated not only around the antenna, but also along with the ECR regions in the configurations shown in Figures 2(b) and 2(c). These computational results clearly suggest that the ion generation is localized in the vicinity of the antenna for the configuration such that the antenna and the magnets are located in parallel direction. This is due to the fact that ECR condition, which traps electrons, is not satisfied on the y=54 plane with the parallel configuration. This is supported by the fact that the spatial distribution of ion generation location is similar to that of electron density. It was also suggested that the ion generation area depends mainly on the antenna direction, while metal boundaries hardly affect the spatial distribution of electrons.

Figure 3 shows the total number of generated ions for each configuration shown in Figures 1(b) to 1(d). As shown in Figure 2, the total number of ions generated in the parallel configuration is much less than those calculated in the perpendicular configurations. It is also identified that the number of generated ions in the two perpendicular configurations are identical by 5.1E-9 seconds(time step:3000), however, the ions generated in the horizontal antenna configuration (Figure 1 (c)) increases more than vertical antenna configuration (Figure 1 (d)) after the time step at 3000. The difference observed in the two perpendicular configurations is due probably to the effect of the metal boundaries. From the analytical results of a series of simulations shown above, it was suggested that the rod antenna of μ6 ion engine (Figure 1(a)) is better to bend 90 degree for increasing the number of ions generated.

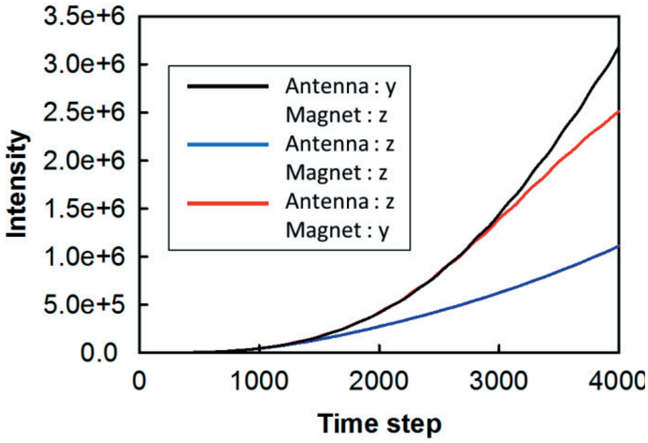

Figure 3 Accumulated number of ions generated in the three configurations.

B. Scattered neutral particle distribution

The spatial distribution of ion generation (or electron density) is analyzed in the previous section. Since ions are generated by the electron impact phenomena, neutral atom density is another important factor to increase the ion generation. One of the points of optimization of ABIE design is to concentrate the neutral atoms into the high electron density area. This is realized by the design of air-intake of ABIE. Statistical compression of the incoming neutral gas atoms is achieved by the narrow collimators located at the air-intake of ABIE. The effect of narrow collimators is confirmed by the previous experiment[8]. Another approach is the focusing of the reflected neutral atoms at the reflector surface. According to the basic design of ABIE previously proposed, the incoming atoms need to be reflected before entering the discharge chamber (see Figure 1(a)). The mean free paths in sub-LEO environment and the discharge chamber at 10^{-2} and 10^{-1} Pa are calculated to be in the order of 3 and 0.3 m at 1500 K. Compared with the diameter of discharge chamber (6 cm), collisions between neutral atoms in the ABIE could be ignored. Therefore, the design of reflector should be based simply on the physics of gas-surface scattering in the hyperthermal velocities.

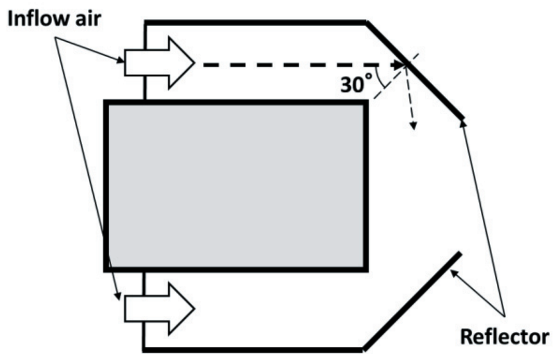

Figure 4. ABIE model used for the neutral gas density calculations.

Scattering event at the solid surface in the hyperthermal energy range has been studied by some research groups. It was widely recognized that the hyperthermal scattering processes of neutral atoms at solid surface has two pathways: direct inelastic scattering (IS) and trapping desorption (TD)[13]. In the IS process, the incoming atoms lose a part of translational energy in the scattering event and eject from the surface with hyperthermal energies. In contrast, the atoms lose all of their energies and thermalized in the TD process. It was reported that the TD process becomes dominant in the small incident angles (close to the normal incidence)[14]. In the TD process flux of the scattered atoms follows cosine distribution (flux at the normal direction is the maximum). This is the case for ABIE. Neutral gas density was calculated with the ABIE model shown in Figure 4 under TD process. The incident angle of the incoming atoms is 30° for this calculation. The snap shots of the spatial distribution of the neutral atoms scattered by the reflector surface are indicated in Figure 5. Figures 5(a) and 5(b) are computational results at the 3000th and 6000th steps. It is confirmed that the neutral gas density increased at the center of the discharge chamber where electron-neutral collision is expected. Moreover, thermalized atoms at the reflector surface are expected to accommodate longer in the ECR region which leads to higher collision probability with electrons trapped in ECR region. As a result, high-efficiency of the ECR plasma formation could be expected.

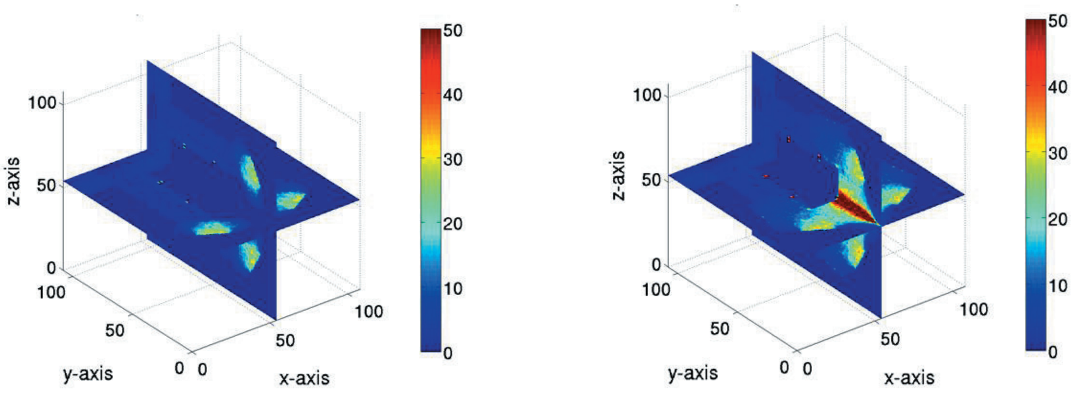

Figure 5 Snap shots of the spatial distribution of the neutral atoms scattered by the reflector surface at 3000th step (a) and 6000th step (b).

IV. Conclusions

In order to optimize the design of ABIE, ECR plasma was numerically simulated using computational code EMSES which has been developed for spacecraft-space plasma interactions. It was suggested that the perpendicular configuration of antenna and magnet increases the ion generation. The effect of metal boundaries was observed after the ECR plasma formation. Neutral scattering event at the reflector surface of ABIE was also simulated. It was analyzed that the use of trapping desorption process is advantageous for ABIE.

Acknowledgments

A part of this work was supported by the Grant-in-Aids from Japan Society for Promotion of Science contract number #25289307, #26289322, 15K14252 and 15K14253. Computation in this study was carried out at the Institute for Information Management and Communication, Kyoto University and Nagoya University.

References

[1]Nishiyama, K., "Air Breathing Ion Engine Concept" *Proceedings of the 54th International Astronautical Congress,* International Astronautical Federation, Paris, 2003; also Paper IAC-03-S4-02.

[2]Nishiyama, K., "Air Breathing Ion Engine" *Proceedings of the 24th International Symposium on Space Technology and Science*, The Japan Society for Aeronautical and Space Science, Tokyo, 2004; also ISTS Paper 2004-o3-05V.

[3]Fujita, K., "Air Intake Performance of Air Breathing Ion Engines," *Journal of the Japan Society for Aeronautical and Space Sciences*, Vol. 52, No. 610, 2004, pp. 514–521. doi:10.2322/jjsass.52.514

[4]Fujita, K., “Air-intake Performance Estimation of Air-breathing Ion Engines” *Journal of the Japan Society of Mechanical Engineers*, Part B, 2004, pp. 3038– 3044.

[5]Schonherr, T., Komurasaki, K., Herdrich, G., “Analysis of Atmosphere-Breathing Electric Propulsion”, *Proceedings of the 33th International Electric Propulsion Conference*, Washington, D.C., 2013; also IEPC Paper 2013-421.

[6]Kirtley, D., Slough, J., Pihl, C., Meier, E., Milroy, R., “Pulsed Plasmoid Propulsion: Air-Breathing Electromagnetic Propulsion”, *Proceedings of the 32th International Electric Propulsion Conference*, Wiesbaden, 2011; also IEPC Paper 2011-015.

[7]Diamant K. D., “A 2-Stage Cylindrical Hall Thruster for Air Breathing Electrical Propulsion,” *46th AIAA/ASME/SAE/ASEE Jount Propulsion Conference and Exhibit*, Nashville, TN, AIAA 2010-6522.

[8]Tagawa, M., Nishiyama, K., Yokota, K., Yoshizawa, Y., Yamamoto, D., Tsuboi, T., Kuninaka, H., “Experimental study of an air breathing ion engine using laser detonation beam source” *J. Propulsion and Power*, Vol.29, 2013, pp.501-506.

[9]Hisamoto, Y., Nishiyama, K, Kuninaka, H., “Characteristics of Hyperthermal Atomic Oxygen Source Using Electron Cyclotron Resonance Discharge and Neutralization Grid”, *Transactions of The Japan Society for Aeronautical and Space Sciences*, Aerospace Technology Japan Vol. 12, 2014, pp.43-48.

[10]Garrigues, L., “Computational Study of Hall-Effect Thruster with Ambient Atmospheric Gas as Propellant”, *Journal of Propulsion and Power*, Vol. 28, No. 2, 2012, pp. 344-354.

[11]Miyake, Y., Usui, H., “New electromagnetic particle simulation code for the analysis of spacecraft-plasma interactions” *Physics of Plasmas*, Vol.16, 2009

[12]Motoyama T, Usui H, Miyake Y, Yokota K, Tagawa M, “Microwave plasma simulation for the development of air breathing ion engine“, *Proceedings of the 29th International Symposium on Space Technology and Science*, The Japan Society for Aeronautical and Space Science, Nagoya, 2013.

[13]Minton, T.K., Giapis, K.P., Moore, T., “Inelastic scattering dynamics of hyperthermal fluorine atoms on a fluorinated silicon surface”, *J. Phys. Chem.A*, 101 (36), 1997, pp. 6549–6555

[14]Minton, T.K., Tagawa, M., Nathanson, G.M., “Energy Accommodation in Hyperthermal Gas-Surface Collisions”,*J. Spacecraft Rockets*, Vol.41, 2004, pp. 389–396